ACS Energy LETTERS

Editors' Choice

http://pubs.acs.org/journal/aelccp

Electrochemical Li Recovery from Spent $LiFePO_4$-Based Li-Ion Batteries

Do-Hwan Nam, Brian M. Foster, and Kyoung-Shin Choi*

Cite This: *ACS Energy Lett.* 2025, 10, 2934−2941

Read Online

ACCESS | Metrics & More | Article Recommendations | Supporting Information

ABSTRACT: **The increase in electric vehicles (EVs) powered by lithium-ion batteries (LIBs) will generate a massive number of spent LIBs in the future. $LiFePO_4$ has recently become the most desired cathode for LIBs in EVs because it is remarkably cheaper and safer than other cathodes. Recovering lithium from spent $LiFePO_4$ batteries using conventional methods, however, may not be economically viable because there are no valuable metals to recover in $LiFePO_4$ other than lithium. This study reports the invention of an electrochemical system, composed of a Li^+-extraction cell and a Li^+-recovery cell, which can recycle Li^+ from spent $LiFePO_4$-LIBs as Li_3PO_4, Li_2CO_3, or LiOH using simple and cost-effective procedures. While recovering Li^+, these cells also regenerate the acid consumed for Li^+ leaching, minimizing the chemicals needed and the waste generated, enabling sustainable and environmentally benign Li^+ recycling. The choice of electrodes, operation principles, performance, and variation of the Li^+-extraction/recovery cells are reported.**

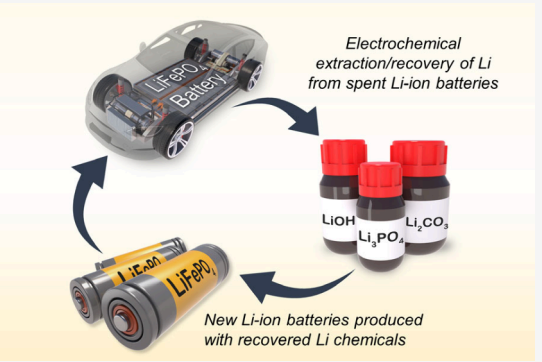

The use of electric vehicles (EVs) enabling carbon-free transportation has significantly increased over the past decade, and it will continue to increase.[1] Most EVs employ lithium-ion batteries (LIBs) to power them owing to their high energy density and high operating voltage. LIBs are also critical in other applications, including energy storage systems (ESSs) that store electrical energy generated from intermittent renewable sources like solar and wind.[2]

The most commonly used cathode materials in LIBs include lithium cobalt oxide ($LiCoO_2$), lithium manganese oxide ($LiMn_2O_4$), lithium nickel manganese cobalt oxide ($LiNi_xMn_yCo_zO_2$), and lithium iron phosphate ($LiFePO_4$).[3,4] Initially, $LiFePO_4$ was considered inferior to Ni- and Co-based cathodes due to its relatively low capacity, low energy density, low operating voltage, poor electronic conductivity, and limited rate capability.[5,6] However, $LiFePO_4$ electrodes are remarkably cheaper than Ni- and Co-based electrodes. Also, their excellent thermal/chemical stability can mitigate the risks of thermal runaway or combustion of battery packs, especially under high-temperature conditions or during overcharging.[7] These unique advantages combined with its outstanding cyclability enabling thousands of charge/discharge cycles make $LiFePO_4$ the most cost-effective and safest cathode for LIBs.[8,9] Consequently, major automakers have transitioned to using $LiFePO_4$ in their EVs.[10] $LiFePO_4$ batteries are projected to occupy a larger market share with the global $LiFePO_4$ market estimated to reach $35.5 billion by 2028.[11]

The continuously growing usage of $LiFePO_4$ will inevitably result in the generation of a massive amount of spent $LiFePO_4$-based LIBs in the future.[10−12] Thus, Li recovery from spent $LiFePO_4$-LIBs is vital to ensure a sustainable Li supply while minimizing negative environmental impacts associated with Li supply and disposal.[13] Current methods for recovering Li from spent LIBs include pyrometallurgy and hydrometallurgy, each with their limitations.[3,14] Pyrometallurgy is energy-intensive and has a low Li recovery rate.[15] Hydrometallurgy involves an extensive series of steps, each consuming various excess chemicals and generating significant waste.[16] A particular challenge with recovering Li from spent $LiFePO_4$-LIBs is that unlike Co/Ni/Mn-based cathodes, there are no other valuable metals to recover other than Li. Thus, the recovery of Li from spent $LiFePO_4$-LIBs using conventional methods may not be economically compelling.

Here, we present a new electrochemical method that can recover Li^+ from spent $LiFePO_4$-LIBs as Li_3PO_4, Li_2CO_3, or LiOH under ambient temperature and pressure conditions while minimizing the chemicals needed for, and the waste

Received: April 8, 2025
Revised: May 17, 2025
Accepted: May 19, 2025
Published: June 4, 2025

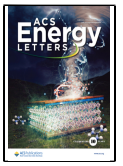

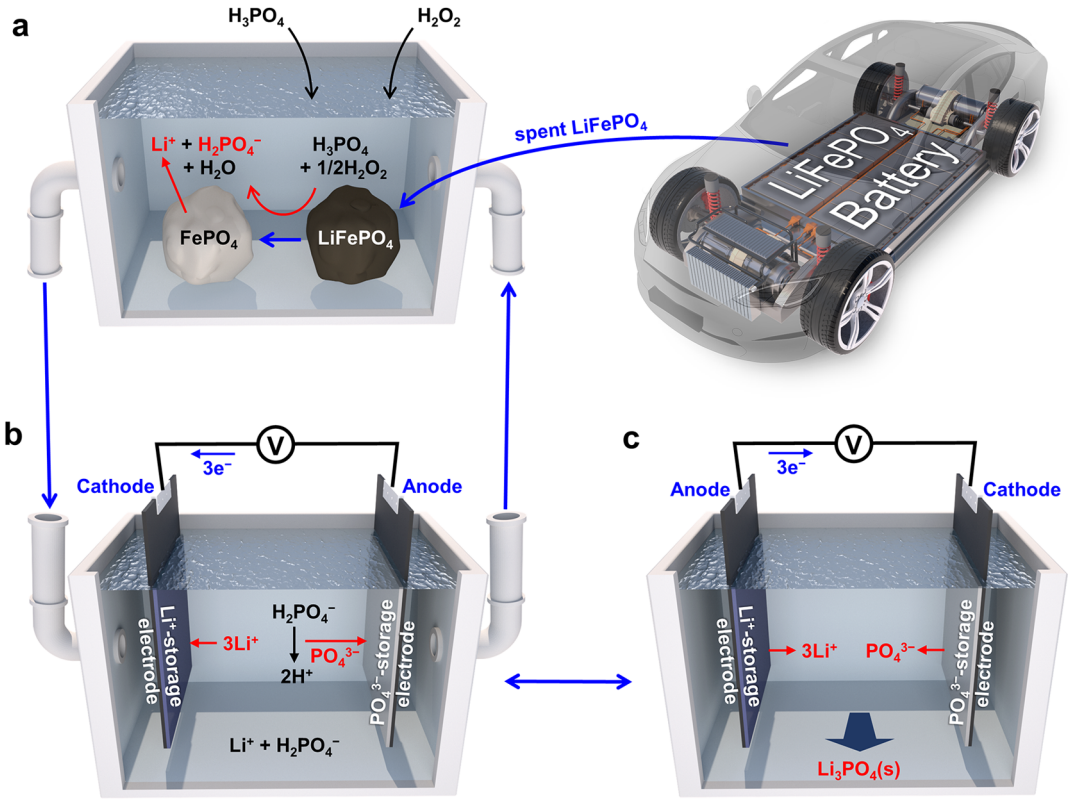

Figure 1. Illustrations of (a) chemical leaching of Li^+ from $LiFePO_4$ using H_3PO_4 and H_2O_2, (b) an electrochemical Li^+-extraction cell composed of a Li^+-storage electrode and a PO_4^{3-}-storage electrode, and (c) an electrochemical Li^+-recovery cell where the extracted Li^+ and PO_4^{3-} are recovered as Li_3PO_4.

generated from, the Li^+-recycling process, which includes the regeneration of acids consumed during the Li^+-leaching step. The multiple advantages provided by our electrochemical process may make Li recovery from spent $LiFePO_4$-LIBs economically viable and sustainable. We describe the operating principles of the electrochemical Li^+-extraction/recovery process, discuss the choices of the electrodes, and demonstrate the performance of the cell.

Operating Principle. Our electrochemical process consists of three steps: (i) chemical leaching of Li^+ from $LiFePO_4$ to an aqueous leachate solution, (ii) electrochemical extraction of Li^+ from the aqueous leachate solution, and (iii) electrochemical recovery of Li^+ as desired chemicals.

The first chemical leaching process of Li^+ from $LiFePO_4$ is performed in an aqueous solution containing an acid and H_2O_2 as an oxidant (Figure 1a), where Fe^{2+} in $LiFePO_4$ is oxidized to Fe^{3+} forming $FePO_4$ (Figure S1), resulting in Li^+ leaching to the solution (eq 1).[17,18] Under mild acidic conditions (pH 3−4), $FePO_4$ is insoluble and the leachate solution contains only Li^+ (Figure S2). However, at pH lower than 3, $FePO_4$ starts to dissolve and introduce Fe ions into the leachate solution (Figure S2).[19] Thus, a pH range of 3−4 was identified as optimal for Li^+ leaching.

$$LiFePO_4(s) + H^+ + 0.5H_2O_2 \rightarrow FePO_4(s) + Li^+(aq) + H_2O \quad (1)$$

Our method uses H_3PO_4 to produce the H^+ needed for the leaching step. Thus, the leaching process can be redescribed as eq 2, and the resulting leachate solution will contain Li^+ and $H_2PO_4^-$, equivalent to a LiH_2PO_4 solution.

$$LiFePO_4(s) + H_3PO_4(aq) + 0.5H_2O_2 \rightarrow FePO_4(s) + H_2PO_4^-(aq) + Li^+(aq) + H_2O \quad (2)$$

As described below, our extraction/recovery step of Li^+ is coupled with the extraction/recovery step of PO_4^{3-}. As a result, the anion part of the acid not consumed for the leaching step is recovered as H_3PO_4 or Li_3PO_4 instead of generating waste. Also, recovered H_3PO_4 minimizes the net amount of acid needed for the leaching step.

After Li^+ leaching from $LiFePO_4$, Li^+ is extracted from the LiH_2PO_4 solution in a Li^+-extraction cell (Figure 1b). The Li^+-extraction cell is composed of a Li^+-storage electrode and a PO_4^{3-}-storage electrode, which selectively extract Li^+ and PO_4^{3-}, respectively, from the leachate solution. When the Li^+-storage electrode and PO_4^{3-}-storage electrode are fully lithiated and phosphatated, respectively, they are moved to a Li^+-recovery cell where the Li^+-storage electrode and PO_4^{3-}-storage electrode release Li^+ and PO_4^{3-}, respectively (Figure 1c). The released Li^+ and PO_4^{3-} are concentrated and precipitate as Li_3PO_4(s) in the appropriate combination of pH and concentrations of Li^+ and PO_4^{3-} (Figure S3).

Choice of Electrodes. The critical components enabling our Li^+-extraction/recovery cells are a Li^+-storage electrode and a PO_4^{3-}-storage electrode that can selectively extract and release Li^+ and PO_4^{3-}, respectively, by the redox reactions of the electrodes without losing their capacity and reversibility for long-term use. Fortunately, it was discovered in our previous study that Bi can serve as a PO_4^{3-}-storage electrode using its electrochemical conversion between Bi and $BiPO_4$ (eq 3): the forward reaction enables PO_4^{3-} storage by Bi, and the reverse reaction enables PO_4^{3-} release by $BiPO_4$.[20] We showed that

https://doi.org/10.1021/acsenergylett.5c01087
ACS Energy Lett. 2025, 10, 2934−2941

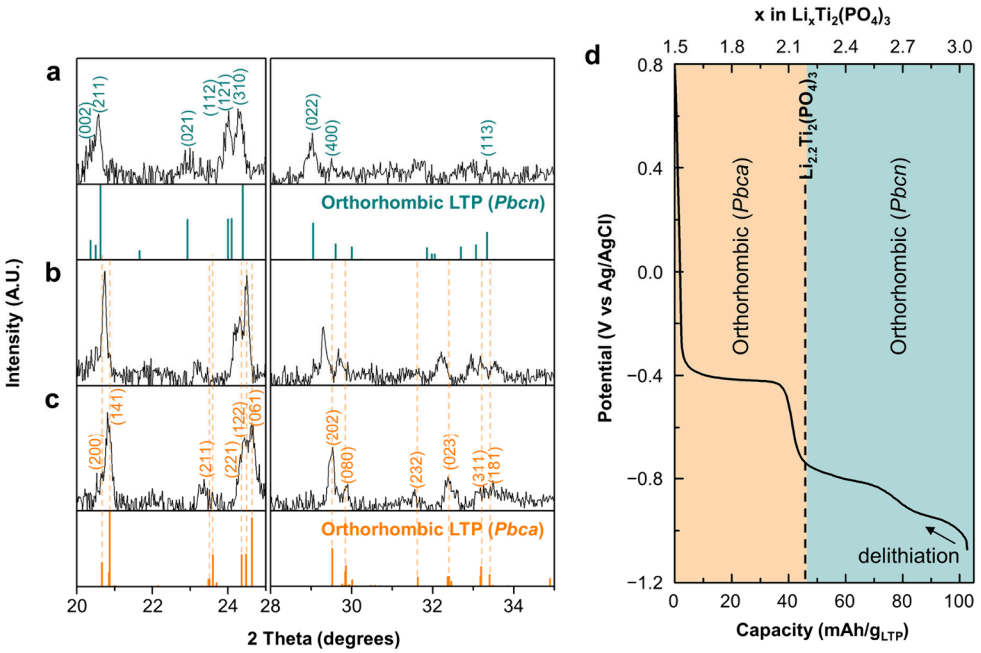

Figure 2. XRD patterns of orthorhombic LTP when (a) fully lithiated at −1.1 V, (b) partially delithiated at −0.65 V, and (c) fully delithiated at 0.8 V vs Ag/AgCl. The difference in peak positions between panels b and c is due to the difference in the Li content affecting the cell parameters of the same *Pbca* structure. (d) Potential−capacity plot obtained in 0.5 M Li_2SO_4 solution during delithiation of fully lithiated orthorhombic LTP at 200 mA/g_{LTP} using −1.1 and 0.8 V vs Ag/AgCl as cutoff potentials.

PO_4^{3-} can be stored not just on the surface of the Bi electrode but also within the bulk of the Bi electrode and that the Bi electrode shows an excellent electrochemical cycle performance for the PO_4^{3-}-storage/release reaction (Figure S4).

$$Bi(s) + H_2PO_4^-(aq) \rightleftharpoons BiPO_4(s) + 2H^+ + 3e^- \quad (3)$$

Thus, the success of our electrochemical Li^+-extract/recovery cells critically depends on the discovery of a suitable Li^+-storage electrode. While there are numerous Li^+-storage electrodes developed for LIB applications, the requirements for a Li^+-storage electrode used in the Li^+-extraction/recovery cells are quite different from those used in LIBs. First, it must be chemically stable in aqueous media in a wide pH range (e.g., acidic for the extraction cell and basic for the recovery cell). Second, the lithiation and delithiation potentials must lie between the water reduction and water oxidation potentials so that the Li^+-extraction/release reactions can occur in aqueous solutions without inducing water reduction and oxidation. Third, it should have excellent electrochemical cycle performance in both acidic and basic aqueous solutions for practical applications. We note that unlike LIB applications, the energy density or powder density is not a critical consideration for the Li^+-storage electrode used in Li^+-extract/recovery cells because they are not energy storage devices.

While some Li^+-storage electrodes used in LIBs can meet the second criterion, Li^+-storage electrodes that are stable in both acidic and basic solutions are rare. However, we discovered that a NASICON-based lithium titanium phosphate ($Li_xTi_2(PO_4)_3$, LTP in short) is exceptionally stable in both aqueous acidic and basic media while satisfying the second criterion. Unfortunately, LTP, which is typically obtained with a rhombohedral structure ($R\bar{3}c$) and undergoes the lithiation/delithiation reactions described in eq 4, has not shown good cycle performance in aqueous media.[21]

$$LiTi_2(PO_4)_3(R\bar{3}c) + 2Li^+ + 2e^- \rightleftharpoons Li_3Ti_2(PO_4)_3(R\bar{3}) \quad (4)$$

Interestingly, we found that $Li_xTi_2(PO_4)_3$ has been synthesized with orthorhombic structures when x is between 1.5 and 3: orthorhombic (*Pbca*) with $1.5 < x < 2.2$ and orthorhombic (*Pbcn*) with $2.2 \leq x \leq 3$.[22,23] These orthorhombic phases cannot be obtained by electrochemically changing the Li content in rhombohedral LTP.[24] Instead, they must be synthesized as orthorhombic LTP from the beginning with the incorporation of an appropriate Li content ($x \geq 1.5$).

To examine whether orthorhombic LTP can have better cycle performance than rhombohedral LTP, we synthesized orthorhombic LTP with the space group *Pbca,* which was confirmed by X-ray diffraction (Figure S5). This orthorhombic LTP powder was mixed with Super C65 as a conducting agent and PTFE as a binder to produce sheet-type LTP electrodes, which is mechanically robust to deal with the constantly changing feedwater and recovery water in Li^+-extraction/recovery processes.

We found that orthorhombic LTP can be fully lithiated at approximately −1.1 V versus Ag/AgCl, and XRD analysis showed that fully lithiated LTP has an orthorhombic (*Pbcn*) structure with an expected formula of $Li_3Ti_2(PO_4)_3$ (Figure 2a). Figure 2d shows the potential−capacity plot of fully lithiated LTP during delithiation at 200 mA/g_{LTP} in a 0.5 M Li_2SO_4 solution. This plot shows three potential plateaus at −1.0, −0.8, and −0.4 V vs Ag/AgCl. XRD analysis showed that the structural transition from *Pbcn* to *Pbca* occurred at the potential between the plateaus at −0.8 V and −0.4 V vs Ag/AgCl (Figure 2b). The potential−capacity plot also shows that delithiation is completed at 0.8 V versus Ag/AgCl, and the XRD analysis shows that the fully delithiated LTP still has a *Pbca* structure (Figure 2c). This indicates that delithiation of orthorhombic LTP does not induce a phase transformation to rhombohedral LTP. The theoretical capacity of LTP (eq 4)

https://doi.org/10.1021/acsenergylett.5c01087
ACS Energy Lett. 2025, 10, 2934−2941

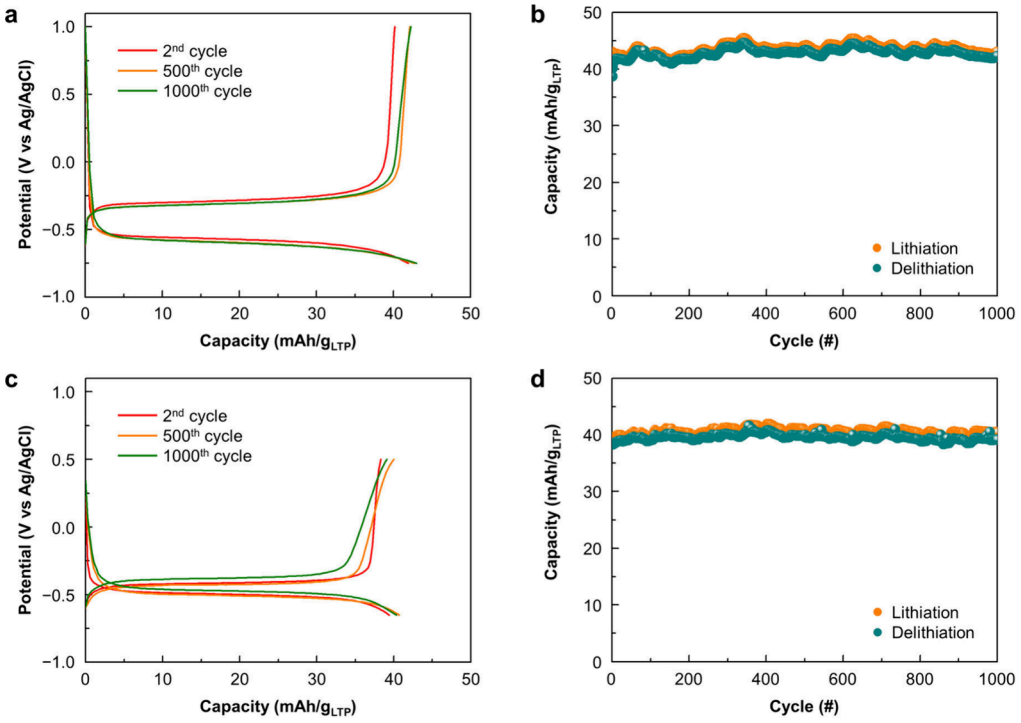

Figure 3. (a) Potential−capacity plots and (b) cyclability of the orthorhombic (*Pbca*) LTP electrode at 200 mA/g_{LTP} in 0.5 M LiH_2PO_4 (pH 3) with cutoff potentials of −0.75 and 1.0 V vs Ag/AgCl. (c) Potential−capacity plots and (d) cyclability of the orthorhombic (*Pbca*) LTP electrode at 200 mA/g_{LTP} in 1 M LiOH (pH 14) with cutoff potentials of −0.65 and 0.5 V vs Ag/AgCl.

with x varying between 1 and 3 is 138.3 mAh/g_{LTP}. However, the observed delithiation capacity was 102 mAh/g_{LTP} and this is very close to the theoretical capacity expected for x varying between 1.5 and 3 (102.8 mAh/g_{LTP}). Thus, the XRD analysis and the observed capacity suggest that lithiation/delithiation of orthorhombic LTP occurs only within the x range that can stabilize orthorhombic structures ($1.5 \leq x \leq 3$), which can be described in eq 5.

$$Li_{1.5}Ti_2(PO_4)_3(Pbca) + 1.5Li^+ + 1.5e^- \rightleftharpoons Li_3Ti_2(PO_4)_3(Pbcn) \quad (5)$$

When the x-value is shown as the top x-axis in the capacity−potential plot (Figure 2d), x = 2.2, where the transition between *Pbca* and *Pbcn* was reported to occur in the previous study,[22] lies between the first (at −0.4 V vs Ag/AgCl) and second (−0.8 V vs Ag/AgCl) potential plateaus, and this agrees well with our own XRD data shown in Figure 2a−c.

Using this information, we performed cycle tests of the orthorhombic LTP using two different potential conditions. The first is to perform lithiation/delithiation cycles to fully utilize the orthorhombic LTP capacity described in eq 5 using cutoff potentials of −1.1 and 1.0 V vs Ag/AgCl, which induces the phase transition between *Pbca* and *Pbcn*. The second is to utilize only the capacity of orthorhombic (*Pbca*) LTP described in eq 6, using the cutoff potentials of −0.75 and 1.0 V vs Ag/AgCl. This potential range covers only the first plateau region (orange region in Figure 2d) and therefore does not induce a structural transformation to *Pbcn*.

$$Li_{1.5}Ti_2(PO_4)_3(Pbca) + 0.7Li^+ + 0.7e^- \rightleftharpoons Li_{2.2}Ti_2(PO_4)_3(Pbca) \quad (6)$$

For the former case, the potential−capacity plots obtained in a near neutral sulfate solution (0.5 M Li_2SO_4) show considerable changes over 700 cycles (Figure S6), suggesting that this operating condition cannot ensure stable cycle performance of LTP for the thousands of cycles in acidic and basic solutions relevant to real applications. However, for the latter case, negligible changes in the potential−capacity profiles are observed over 1000 cycles in 0.5 M LiH_2PO_4 (pH 3) that mimics the acidic leachate solution (Figure 3a,b).

We also performed a cycle test in highly alkaline 1 M LiOH (pH 14) using only the capacity of orthorhombic (*Pbca*) LTP and observed a stable cycle performance over 1000 cycles (Figure 3c,d), which is remarkable. These results show that when LTP is synthesized with the orthorhombic (*Pbca*) structure and its lithiation capacity is regulated so that the *Pbca* structure is retained, LTP becomes an excellent candidate for our electrochemical Li^+-extraction/recovery system. Performing lithiation/delithiation in eq 6 where x varies only between 1.5 and 2.2 reduces the specific capacity of LTP (~48 mAh/g_{LTP}). However, the resulting electrochemical stability and cyclability in both acidic and basic aqueous media are exceptional and cannot be accessed by other Li^+-storage materials. Also, the low specific capacity is not of concern for our system as it is not an energy-storage device.

Performance of the LTP/Bi Cell for Li^+ Extraction and Its Recovery as Li_3PO_4. We now couple the LTP electrode and the Bi electrode to show the operation of the LTP/Bi cell for Li^+ extraction and recovery. In the Li^+-extraction cell (Figure 1b), LTP storing Li^+ via the reduction of Ti^{4+} to Ti^{3+} serves as the cathode and Bi storing PO_4^{3-} via the oxidation of Bi to Bi^{3+} serves as the anode in 0.5 M LiH_2PO_4 that mimics the solution obtained by Li^+ leaching in H_3PO_4 (eq 2). As the potential−capacity profile and excellent cycle performance of the LTP electrode in this solution are already presented in

https://doi.org/10.1021/acsenergylett.5c01087
ACS Energy Lett. 2025, 10, 2934−2941

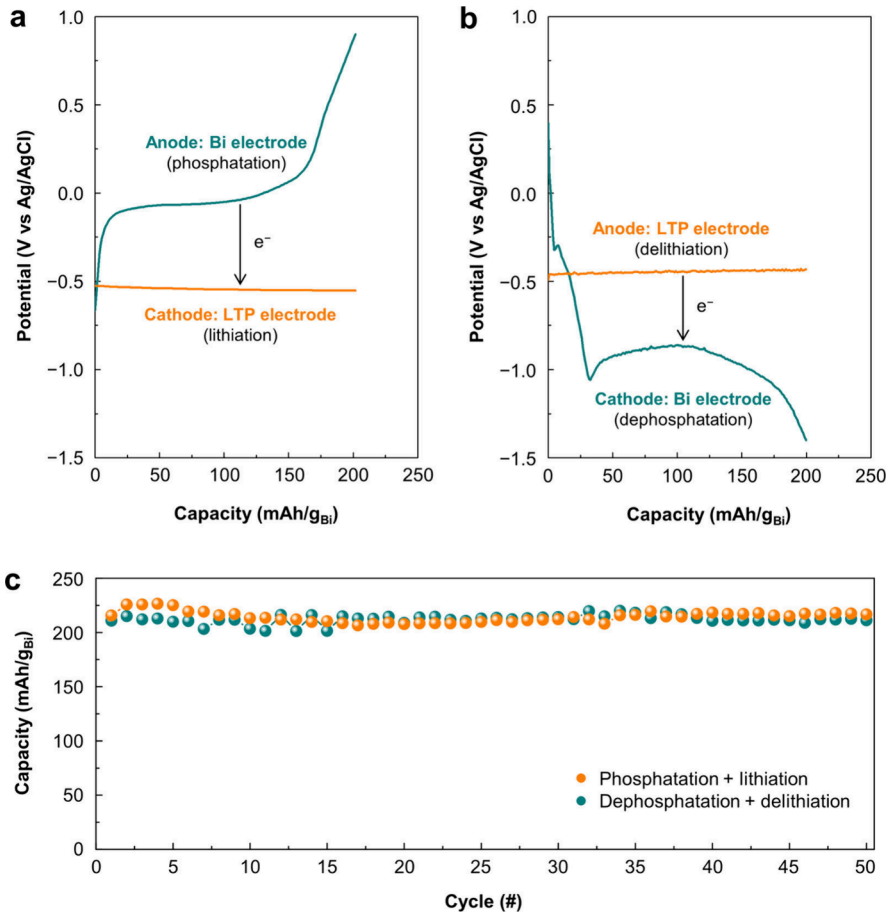

Figure 4. Potential−capacity plots of the orthorhombic (*Pbca*) LTP electrode and Bi electrode for (a) Li^+ extraction in 0.5 M LiH_2PO_4 and (b) Li^+ recovery in 0.5 M LiCl at ±770 mA/g_{Bi}, with cutoff potentials of 0.9 V and −1.4 V vs Ag/AgCl. (c) Cycling tests of Li^+ extraction in 0.5 M LiH_2PO_4 and Li^+ recovery in 0.5 M LiCl for 50 cycles.

Figure 3, we operated the LTP/Bi cell using the Bi electrode as the working electrode, so that its electrochemical behavior coupled with the LTP counter electrode in 0.5 M LiH_2PO_4 can be examined.

Figure 4a shows the potential profiles of the LTP and Bi electrodes in the Li^+-extraction cell when it was operated at 770 mA/g_{Bi} (2 C-rate based on the theoretical capacity of Bi) using 0.9 V and −1.4 V vs Ag/AgCl of the Bi electrode as the cutoff potentials. The average potential difference between the cathode and the anode was 0.6 V, and the phosphatation capacity of the Bi electrode was 210.95 mAh/g. The Faradaic efficiency for Li^+ extraction by the LTP electrode was ∼91%, and that for PO_4^{3-} extraction by the Bi electrode was ∼100% (Table S2), determined by quantifying the actual Li^+ and PO_4^{3-} removed from the solution. The lower Li^+-extraction efficiency of the LTP electrode is likely due to the self-discharge reaction, wherein LTP undergoes spontaneous oxidation upon reacting with O_2 in the electrolyte.[25]

Once the LTP and Bi electrodes are saturated with Li^+ and PO_4^{3-}, respectively, they are transferred to the Li^+-recovery cell (Figure 1c). In this cell, LTP releasing Li^+ by the oxidation of Ti^{3+} to Ti^{4+} serves as the anode and $BiPO_4$ releasing PO_4^{3-} by the reduction of Bi^{3+} to Bi serves as the cathode. The concentrated Li^+ and PO_4^{3-} in the Li^+-recovery cell precipitate as Li_3PO_4 when their concentrations exceed their solubility limit (K_{sp} of $Li_3PO_4 = 3.2 \times 10^{-9}$) (Figure S3). We used 0.5 M LiCl as the electrolyte for the Li^+-recovery cell as LiCl would not affect the purity of Li_3PO_4 collected while offering the needed solution conductivity. Figure 4b shows the potential−capacity profiles of both electrodes in the Li^+-recovery cell operating at a current density of 770 mA/g_{Bi}. Initially, the cathode potential is more positive than the anode potential, indicating a positive E_{cell} and energy output from the Li^+-recovery cell (the reaction occurs spontaneously). However, as the reaction progresses and the required overpotentials increase, the cathode potential becomes more negative than the anode potential, and the net reaction is nonspontaneous, necessitating energy input. The Faradaic efficiencies for both Li^+ and PO_4^{3-} recovery by the LTP electrode and Bi electrode were ∼100% (Table S2). The XRD analysis of the white precipitate obtained from the Li^+-recovery cell confirms the formation of high-purity and crystalline Li_3PO_4 (Figure S7).

The potential−capacity plots in Figure 4a,b were used to preliminarily estimate the total energy consumption during operation of the Li^+-extraction/recovery cells. This calculation along with the FE for Li^+ extraction and Li^+ recovery suggests that the total energy required for the production of 1 kg of Li_3PO_4 using our Li^+-extraction/recovery cells is 0.80 kWh. Detailed calculations are provided in Figure S8. As expected from the excellent cycle performances of the individual LTP and Bi electrodes, their combination in the Li^+-extraction/recovery cells also showed excellent cycle performance: the phosphatation capacity of the Bi electrode under the given operating condition (210.95 mAh/g_{Bi}) was maintained without

https://doi.org/10.1021/acsenergylett.5c01087
ACS Energy Lett. 2025, 10, 2934−2941

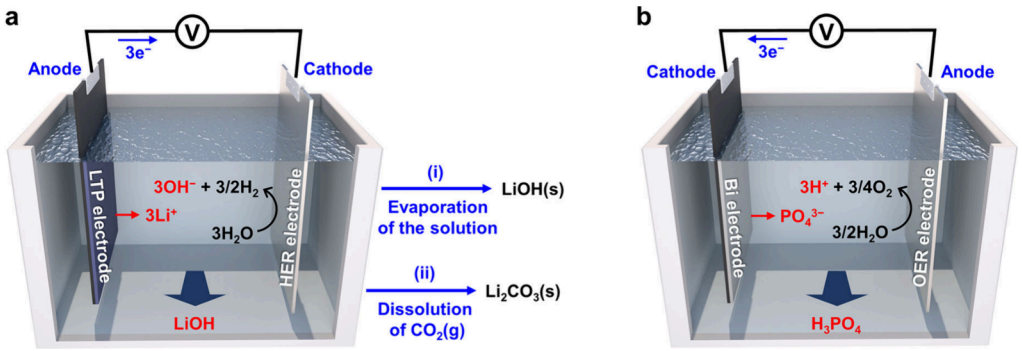

Figure 5. (a) Li^+-recovery cell where Li^+ is recovered as LiOH and (b) PO_4^{3-}-recovery cell where PO_4^{3-} is recovered as H_3PO_4.

any capacity fading during the cycle test (Figure 4c). (Because we currently do not have an automated system, cycling the electrodes between the Li^+-extraction cell and Li^+-recovery cell required manual transfer of the electrodes between the two cells, which limited the number of cycles shown in Figure 4c.)

Recovery of the Extracted Li as LiOH and Li_2CO_3. The remarkable chemical and electrochemical stability of LTP in a strongly basic solution (pH 14) also allows for the recovery of the extracted Li^+ as LiOH or Li_2CO_3 through the modification of the Li^+-recovery cell. In the modified Li^+-recovery cell, the lithiated LTP electrode serving as the anode is coupled with a cathode performing a hydrogen evolution reaction (HER) or an oxygen reduction reaction (ORR) in a dilute LiOH solution. Then Li^+ released from the anode and OH^- produced from the cathode accumulate as concentrated LiOH(aq) (Figure 5a), and solid LiOH powder can be obtained by the evaporation of water (Figure 5i). Alternatively, the concentrated alkaline LiOH solution can be used to capture CO_2(g) as CO_3^{2-}, which precipitates Li^+ as Li_2CO_3 powder without needing an evaporation step (Figure 5ii) (eqs 7 and 8). The XRD patterns of the LiOH(s) and Li_2CO_3(s) we obtained through the operation of such modified Li^+-recovery cells are shown in Figure S9.

$$2OH^- + CO_2 \rightarrow CO_3^{2-} + H_2O \quad (7)$$

$$2Li^+ + CO_3^{2-} \rightarrow Li_2CO_3(s) \quad (8)$$

Regeneration of Acids Consumed during the Li^+-Leaching Step. When the lithiated LTP is coupled with the cathode performing HER or ORR in the modified Li^+-recovery cell, the phosphatated Bi serving as the cathode is coupled with an anode performing the oxygen evolution reaction (OER) in a PO_4^{3-}-recovery cell (Figure 5b). In this cell, phosphatated Bi releases PO_4^{3-} upon reduction, and the anode produces H^+, accumulating H_3PO_4, which will be used for the Li^+-leaching step. The potential−capacity plots of the modified Li^+-recovery cell and the PO_4^{3-}-recovery cell are shown in Figure S10 with preliminary calculations for the energy consumption and cost for the Li^+ recovery as LiOH and the PO_4^{3-} recovery as H_3PO_4.

We note that for the original Li^+-extraction/recovery cells where Li^+ is recovered as Li_3PO_4, 2/3 of H_3PO_4 consumed during the Li^+-leaching step is regenerated as H_3PO_4 in the Li^+-extraction cell and the remaining PO_4^{3-} is recovered as Li_3PO_4 in the Li^+-recovery cell, generating no PO_4^{3-} waste. For the modified Li^+-recovery cell where Li^+ is recovered as LiOH or Li_2CO_3, the remaining PO_4^{3-} is recovered as H_3PO_4 in the PO_4^{3-}-recovery cell, thus fully regenerating all H_3PO_4 consumed during the Li^+-leaching step (2/3 in the Li^+-extraction cell and 1/3 in the PO_4^{3-}-recovery cell). This means regardless of the type of recovered Li chemicals, our electrochemical methods require minimal chemicals and generate minimal waste.

We also note that our electrochemical cell can be modified to use acids other than H_3PO_4 for Li^+ leaching when it is preferred. For example, when H_2SO_4 is used as the acid for Li^+ leaching, the resulting leachate solution will be a Li_2SO_4(aq) solution, and the electrode reactions that will be used in the Li^+-extraction/recovery cells are shown in Figure S11. We confirmed the excellent cycle performance of the LTP electrode (i.e., no capacity fading over 50,000 cycles that took approximately seven months) in 0.5 M Li_2SO_4 solution (Figure S12). As in the case of using H_3PO_4, the H_2SO_4 consumed for Li^+ leaching is regenerated in the Li^+-extraction cell (details in Figure S11 caption).

Li Recovery from Spent $LiFePO_4$-LIBs. We preliminarily confirmed that our method is viable to recover Li^+ from real $LiFePO_4$-LIBs using two experiments. In the first experiment, we obtained and disassembled a commercial $LiFePO_4$-LIB after it was fully discharged. Then we scraped the $LiFePO_4$ electrode composed of $LiFePO_4$, carbon, and binder from the Al current collector, followed by rinsing, grinding, and drying as described in the Supporting Information. The resulting powder was used to leach Li^+, and we operated the Li^+-extraction/recovery cells to recover the extracted Li^+ as high-purity white powders of Li_3PO_4, LiOH, and Li_2CO_3 (Figure S13). The presence of carbon and binder mixed with $LiFePO_4$ powder did not affect the Li^+-leaching process or the purity of the Li chemicals generated by our electrochemical method.

In the second experiment, we obtained a black mass that is industrially mass-produced from spent $LiFePO_4$-LIBs (Ecopro HN) and recovered Li^+ as Li_3PO_4. In current industrial recycling processes for spent LIBs, the batteries are fed into a crushing chamber and then sieved to separate steel scraps and plastic components. The remaining powder is called back mass and is composed of active electrode materials (e.g., $LiFePO_4$ cathode and graphite anode), current collectors (e.g., Cu and Al), conducting agents, and organic compounds (binder, supporting electrolytes, and additives). The collected black mass then undergoes a calcination process to remove organic species that can interfere with the following Li^+-recycling processes. The calcination process of the black mass we obtained was optimized for a hydrometallurgical process (e.g., the decomposition of binders at high temperatures), which is not needed for our process, as the presence of binders has no impact on selective electrochemical Li^+ extraction. Nonethe-

https://doi.org/10.1021/acsenergylett.5c01087
ACS Energy Lett. 2025, 10, 2934−2941

less, we confirmed that our method can extract Li^+ from this unoptimized black mass and recover it as high-purity Li_3PO_4 (Figure S14).

In summary, we have developed an electrochemical method to extract and recover Li^+ from spent $LiFePO_4$-LIBs as Li_3PO_4, LiOH, and Li_2CO_3 under ambient conditions. The anionic parts of these salts are from the acid used for Li^+ leaching, electrochemically derived OH^-, or CO_2 capture, minimizing the chemicals needed to produce these chemicals. Also, the acid used for Li^+ leaching is fully or partially regenerated by the electrochemical reactions in the Li^+-extraction/recovery cells, minimizing the consumption of acid and the generation of salt wastes. The realization of these cells was enabled by synthesizing and understanding lithiation/delithiation properties of orthorhombic LTP, which enabled LTP to have excellent cycle performance in both acidic and basic conditions. The electrochemical method presented in this study opens up a new possibility to recover Li^+ from spent $LiFePO_4$-LIBs in a sustainable and economically viable manner.

■ ASSOCIATED CONTENT

Supporting Information

The Supporting Information is available free of charge at https://pubs.acs.org/doi/10.1021/acsenergylett.5c01087.

Methods, supplementary text (electrode capacity calculations, regeneration of H_3PO_4, energy consumption calculations), results for Li^+ leaching, additional electrochemical and XRD results, additional thermodynamic data, Faradaic efficiencies, and modifications of Li^+-extraction cell (PDF)

■ AUTHOR INFORMATION

Corresponding Author

Kyoung-Shin Choi − *Department of Chemistry, University of Wisconsin−Madison, Madison, Wisconsin 53706, United States;* orcid.org/0000-0003-1945-8794; Email: kschoi@chem.wisc.edu

Authors

Do-Hwan Nam − *Department of Chemistry, University of Wisconsin−Madison, Madison, Wisconsin 53706, United States;* orcid.org/0000-0002-5601-3172

Brian M. Foster − *Department of Chemistry, University of Wisconsin−Madison, Madison, Wisconsin 53706, United States*

Complete contact information is available at: https://pubs.acs.org/10.1021/acsenergylett.5c01087

Notes

The authors declare the following competing financial interest(s): DHN, BMF, and KSC are inventors on a patent related to this work filed by the Wisconsin Alumni Research Foundation.

■ ACKNOWLEDGMENTS

This work was supported by Samsung E&A and the University of Wisconsin−Madison. BMF was supported by the National Science Foundation Graduate Research Fellowship Program under Grant No. 2137424. The authors thank Ecopro HN for providing black mass of spent $LiFePO_4$-LIBs.

■ REFERENCES

(1) Mauler, L.; Duffner, F.; Zeier, W. G.; Leker, J. Battery Cost Forecasting: A Review of Methods and Results with An Outlook to 2050. *Energy Environ. Sci.* **2021**, *14*, 4712−4739.

(2) Degen, F.; Winter, M.; Bendig, D.; Tübke, J. Energy Consumption of Current and Future Production of Lithium-Ion and Post Lithium-Ion Battery Cells. *Nat. Energy* **2023**, *8*, 1284−1295.

(3) Wang, J.; Ma, J.; Zhuang, Z.; Liang, Z.; Jia, K.; Ji, G.; Zhou, G.; Cheng, H.-M. Toward Direct Regeneration of Spent Lithium-Ion Batteries: A Next-Generation Recycling Method. *Chem. Rev.* **2024**, *124*, 2839−2887.

(4) Mauler, L.; Lou, X.; Duffner, F.; Leker, J. Technological Innovation vs. Tightening Raw Material Markets: Falling Battery Costs Put at Risk. *Energy Adv.* **2022**, *1*, 136−145.

(5) Zhang, W.-J. Structure and Performance of $LiFePO_4$ Cathode Materials: A Review. *J. Power Sources* **2011**, *196*, 2962−2970.

(6) Li, Z.; Yang, J.; Guang, T.; Fan, B.; Zhu, K.; Wang, X. Controlled Hydrothermal/Solvothermal Synthesis of High-Performance $LiFePO_4$ for Li-Ion Batteries. *Small Methods* **2021**, *5*, 2100193.

(7) Kvasha, A.; Gutiérrez, C.; Osa, U.; de Meatza, I.; Blazquez, J. A.; Macicior, H.; Urdampilleta, I. A Comparative Study of Thermal Runaway of Commercial Lithium Ion Cells. *Energy* **2018**, *159*, 547−557.

(8) Yuan, L.-X.; Wang, Z.-H.; Zhang, W.-X.; Hu, X.-L.; Chen, J.-T.; Huang, Y.-H.; Goodenough, J. B. Development and Challenges of $LiFePO_4$ Cathode Material for Lithium-Ion Batteries. *Energy Environ. Sci.* **2011**, *4*, 269−284.

(9) Li, J.; Ma, Z.-F. Past and Present of $LiFePO_4$: from Fundamental Research to Industrial Applications. *Chem.* **2019**, *5*, 3−6.

(10) Walvekar, H.; Beltran, H.; Sripad, S.; Pecht, M. Implications of the Electric Vehicle Manufacturers' Decision to Mass Adopt Lithium-Iron Phosphate Batteries. *IEEE Access* **2022**, *10*, 63834−63843.

(11) Lithium Iron Phosphate Batteries Market by Industry (Automotive, Power, Industrial, Consumer Electronics, Aerospace, Marine, Others), Application (Portable, Stationary), Voltage (Low, Medium, High), Capacity, Design, and Region - Global Forecast to 2028. https://www.marketsandmarkets.com/Market-Reports/lithium-iron-phosphate-batteries-market-77659282.html (accessed 2025-05-13).

(12) Wang, W.; Wu, Y. An Overview of Recycling and Treatment of Spent $LiFePO_4$ Batteries in China. *Resour. Conserv. Recycl.* **2017**, *127*, 233−243.

(13) Arshad, F.; Lin, J.; Manurkar, N.; Fan, E.; Ahmad, A.; Tariq, M-u.-N.; Wu, F.; Chen, R.; Li, L. Life Cycle Assessment of Lithium-Ion Batteries: A Critical Review. *Resour. Conserv. Recycl.* **2022**, *180*, 106164.

(14) Recycle Spent Batteries. *Nat. Energy* **2019**, *4*, 253.

(15) Cornelio, A.; Zanoletti, A.; Bontempi, E. Recent Progress in Pyrometallurgy for the Recovery of Spent Lithium-Ion Batteries: A Review of State-of-the-Art Developments. *Curr. Opin. Green Sustain. Chem.* **2024**, *46*, 100881.

(16) Jung, J. C.-Y.; Sui, P.-C.; Zhang, J. A Review of Recycling Spent Lithium-Ion Battery Cathode Materials Using Hydrometallurgical Treatments. *J. Energy Storage* **2021**, *35*, 102217.

(17) Li, H.; Xing, S.; Liu, Y.; Li, F.; Guo, H.; Kuang, G. Recovery of Lithium, Iron, and Phosphorus from Spent $LiFePO_4$ Batteries Using Stoichiometric Sulfuric Acid Leaching System. *ACS Sustain. Chem. Eng.* **2017**, *5*, 8017−8024.

(18) Yang, Y.; Meng, X.; Cao, H.; Lin, X.; Liu, C.; Sun, Y.; Zhang, Y.; Sun, Z. Selective Recovery of Lithium From Spent Lithium Iron Phosphate Batteries: A Sustainable Process. *Green Chem.* **2018**, *20*, 3121−3133.

(19) Jing, Q.; Zhang, J.; Liu, Y.; Yang, C.; Ma, B.; Chen, Y.; Wang, C. E-pH Diagrams for the Li-Fe-P-H_2O System from 298 to 473 K: Thermodynamic Analysis and Application to the Wet Chemical Processes of the $LiFePO_4$ Cathode Material. *J. Phys. Chem. C* **2019**, *123*, 14207−14215.

(20) Nam, D.-H.; Choi, K.-S. Electrochemical Bi/$BiPO_4$ Cells for a Sustainable Phosphate Cycle. *ACS Energy Lett.* **2023**, *8*, 802−808.

(21) Xu, T.; Zhao, M.; Su, Z.; Duan, W.; Shi, Y.; Li, Z.; Pol, V. G.; Song, X. Nanostructured $LiTi_2(PO_4)_3$ Anode with Superior Lithium and Sodium Storage Capability Aqueous Electrolytes. *J. Power Sources* **2021**, *481*, 229110.
(22) Wang, S.; Hwu, S.-J. A New Series of Mixed-Valence Titanium (III/IV) Phosphate, $Li_{1+x}Ti_2(PO_4)_3$ ($0 \leq x \leq 2$), with NASICON-Related Structures. *Chem. Mater.* **1992**, *4*, 589−595.
(23) Wang, S.; Hwu, S.-J. $Li_{3-x}Ti_2(PO_4)_3$ ($0 \leq x \leq 1$): A New Mixed Valent Titanium (III/IV) Phosphate with a NASICON-Type Structure. *J. Solid State Chem.* **1991**, *90*, 377−381.
(24) Patoux, S.; Masquelier, C. Lithium Insertion into Titanium Phosphates, Silicates, and Sulfates. *Chem. Mater.* **2002**, *14*, 5057−5068.
(25) Li, Z.; Ravnsbaek, D. B.; Xiang, K.; Chiang, Y.-M. $Na_3Ti_2(PO_4)_3$ as a Sodium-Bearing Anode for Rechargeable Aqueous Sodium-Ion Batteries. *Electrochem. Commun.* **2014**, *44*, 12−15.

https://doi.org/10.1021/acsenergylett.5c01087
ACS Energy Lett. 2025, 10, 2934−2941